Role of single-domain magnetic particles in creation of inverse magnetic fabrics in volcanic rocks: A mathematical model study

FRANTIŠEK HROUDA[1,2] AND JOSEF JEŽEK[2]

1 AGICO Ltd., Ječná 29a, Brno, Czech Republic (fhrouda@agico.cz)

2 Faculty of Sciences, Charles University, Albertov 6, 128 43 Praha 2, Czech Republic

Received: September 30, 2015; Revised: January 27, 2016; Accepted: June 24, 2016

ABSTRACT

The role of single-domain (SD) magnetic particles in creation of inverse magnetic fabrics is investigated on simple mathematical models using a realistic estimate for SD intrinsic susceptibility. In contrast to the fraction created by multi-domain (MD) particles, in which the anisotropy of magnetic susceptibility (AMS) is controlled by both the grain AMS and intensity of the preferred orientation of the particles, the AMS of the SD fraction is controlled solely by the intensity of the preferred orientation. The degree of AMS of ensemble of SD grains with a preferred orientation is therefore much higher than that of the same ensemble of MD particles implying the existence of frequent inverse magnetic fabrics. However, the occurrence of inverse magnetic fabrics due to SD particles is more the exception than the rule. Consequently, the amounts of SD particles is probably in general low. Nevertheless, the presence of SD particles in amounts insufficient to create inverse magnetic fabrics may diminish the whole rock AMS substantially. This can be one of the reasons for relatively low AMS in volcanic rocks whose magnetic particles may be really small obeying the conditions for the existence of SD particles.

Keywords: AMS of SD magnetic particles, inverse magnetic fabric, volcanic rocks

1. INTRODUCTION

In most rocks, the magnetic fabric investigated through the anisotropy of magnetic susceptibility (AMS) is concordant with the macroscopic rock fabric, i.e. the magnetic foliation is roughly parallel to the main mesoscopic foliation of whatever origin and the magnetic lineation to the mesoscopic lineation. This magnetic fabric can be termed normal magnetic fabric. In some rocks, the magnetic lineation is perpendicular to the mesoscopic lineation and the magnetic foliation perpendicular to the mesoscopic foliation (e.g., *Graham, 1966*; *Rochette, 1988*; *Ihmlé et al., 1989*; *Winkler et al., 1996*; *Borradaile and Gauthier, 2001*; *Ferré, 2002*; *Chadima et al., 2009*); this magnetic fabric can be termed inverse magnetic fabric. The reasons for the existence of the inverse magnetic fabric may be geological as, for instance, tectonic thickening in deformed rocks (e.g., *Graham, 1966*), special lava flow mechanism in dykes (e.g., *Raposo and Ernesto, 1995*), AMS carried by tourmaline, or cordierite, or iron-bearing carbonates (e.g., *Ihmlé et al., 1989*; *Rochette et al., 1992*) or physical, viz AMS carried by single-domain (SD) magnetic grains (e.g., *Stephenson et al., 1986*).

The inverse magnetic fabric is particularly important in volcanic rocks. Namely, in lava flows, sills, and dykes, whose AMS is carried by multi-domain (MD) titanomagnetite, in which the AMS ellipsoid resembles the ellipsoid-approximated grain shape, the magnetic foliation is often found to be near the flow plane and the magnetic lineation is mostly parallel to the lava flow direction (*Ernst and Baragar, 1992*; *Canon-Tapia et al., 1994*; *Raposo and Ernesto, 1995*; *Hrouda et al., 2002*). Less frequently, the magnetic foliation is roughly perpendicular to the flow plane and the magnetic lineation perpendicular to the lava flow direction, clearly creating the inverse magnetic fabric (e.g., *Raposo and Ernesto, 1995*; *Chadima et al., 2009*). This fabric may be either due to special lava flow regime or, in rocks with normal lava flow regime, due to prevailing representation of magnetic minerals by SD grains, because in these grains the maximum and minimum susceptibilities are oriented inversely with respect to grain shape (*Stephenson et al., 1986*). This dualism can have unpleasant consequences for the interpretation of a particular magnetic fabric. Two tools to discriminate between the inverse magnetic fabric due to special lava flow regime from that due to dominating presence of SD particles were suggested by *Stephenson et al. (1986)* and *Almqvist et al. (2012)*. They consist of the investigation of both AMS and anisotropy of magnetic remanence (AMR) or high-field (torque) magnetic anisotropy (HFA). While the AMS magnetic fabric is inverted in SD particles with respect to MD particles, the AMR or HFA magnetic fabric is always coaxial in MD and SD particles. Consequently, the inverse AMS fabric can be interpreted correctly either in terms of special lava flow regime or in terms of dominating SD particles.

The interplay between mineral fractions with normal and inverse magnetic fabrics was investigated on mathematical models simulating varying proportions of the above fractions (*Rochette et al., 1992, 1999*; *Dragoni et al., 1997*; *Ferré, 2002*). It was found that increasing proportion of mineral fraction with inverse magnetic fabric results in progressively decreasing the intensity of the overall magnetic fabric and vice versa. The orientations of magnetic foliations and magnetic lineations are in general controlled by the prevailing fraction. Intermediate magnetic fabrics, characterized by the parallelism of both the magnetic lineation and magnetic foliation pole to the macroscopic rock foliation, were also revealed.

The present paper extends the above models by estimating the AMS of both the MD and SD magnetite (titanomagnetite) fractions considering the same realistic directional distributions of the axes of both the MD and SD particles as well as realistic intrinsic susceptibilities of theirs. Using this model, the importance of the SD magnetic fabric is investigated as well as the conditions under which the SD fabric only weakens the MD fabric and those under which the SD fabric can dominate the rock magnetic fabric. Partial solutions are suggested to quantitatively assess the effect of SD particles on the whole rock AMS.

2. MODEL OF THE AMS OF MAGNETICALLY MONOMINERALIC ROCK

Theory of the low-field AMS is based on the assumption of the linear relationship between magnetization and magnetizing field, traditionally described in the SI of units, which is used throughout the paper, as follows

$$\boldsymbol{M} = \mathbf{k}\boldsymbol{H} \ , \tag{1}$$

where $\boldsymbol{M}$ is magnetization vector, $\boldsymbol{H}$ is vector of the intensity of external magnetizing field, and $\mathbf{k}$ is symmetric second-rank tensor of apparent or measured magnetic susceptibility. In magnetic fabric studies, the AMS of rocks is conveniently characterized by the following parameters derived from the principal susceptibilities of the $\mathbf{k}$ tensor (e.g., *Nagata, 1961*; *Jelínek, 1981*)

$$k_m = \frac{k_1 + k_2 + k_3}{3} \ , \quad P = \frac{k_1}{k_3} \ , \quad T = \frac{2\eta_2 - \eta_1 - \eta_3}{\eta_1 - \eta_3} \ , \tag{2}$$

where $k_1 \geq k_2 \geq k_3$ are principal susceptibilites and $\eta_1 = \ln k_1$, $\eta_2 = \ln k_2$, $\eta_3 = \ln k_3$. The parameter k_m is the mean susceptibility, P is the degree of AMS and T characterizes the shape of the AMS ellipsoid. If $0 < T < 1$, the AMS ellipsoid is oblate; $T = 1$ means that the AMS ellipsoid is rotational oblate. If $-1 < T < 0$, the AMS ellipsoid is prolate; $T = -1$ means that the AMS ellipsoid is rotational prolate. If $T = 0$, the ellipsoid is neutral.

In general, the rock AMS is controlled by both the grain AMS of the mineral carrying the rock's AMS and the preferred orientation of the mineral (e.g., *Hrouda, 1982*; *Tarling and Hrouda, 1993*). In the AMS models, the grain AMS is usually characterized by the above parameters and the preferred orientation is represented either by Bingham distribution (e.g., *Owens, 1974*) or by Fisher distribution (e.g., *Hrouda, 1980*). Besides, it can be characterized by the orientation tensor **E**, which, for uniaxial magnetic grains, is defined as follows (*Scheidegger, 1965*; *Ježek and Hrouda, 2000*)

$$\mathbf{E} = \frac{1}{n}\begin{pmatrix} \sum_i l_i^2 & \sum_i l_i m_i & \sum_i l_i n_i \\ \sum_i m_i l_i & \sum_i m_i^2 & \sum_i m_i n_i \\ \sum_i n_i l_i & \sum_i m_i n_i & \sum_i n_i^2 \end{pmatrix} \ , \tag{3}$$

where l_i, m_i, n_i are the direction cosines of the i-th grain axis and n is the number of the grains considered. The principal values of the tensor **E** ($E_1 \geq E_2 \geq E_3$) satisfy the condition $E_1 + E_2 + E_3 = 1$. The intensity of the preferred orientation of the grain axes can be characterized by the I parameter introduced by *Lisle (1985)*

$$I = \frac{15}{2}\sum_{i=1}^{3}\left(E_i - \frac{1}{3}\right)^2 \ , \tag{4}$$

where E_i ($i = 1, 2, 3$) are principal values of the orientation tensor. It can vary from 0 for isotropic fabric to 5 for the fabric in which all grain axes are perfectly parallel to one another. The character of the preferred orientation can be characterized by the T_e parameter analogous to the T parameter used in AMS studies

$$T_e = \frac{2 \ln E_2 - \ln E_1 - \ln E_3}{\ln E_1 - \ln E_3} \ . \tag{5}$$

Consequently, $-1 \leq T_e \leq 0$ ($E_1 \gg E_2 > E_3$) represents a cluster type of distribution, whereas $0 < T_e \leq 1$ ($E_1 > E_2 \ll E_3$) corresponds to a girdle type pattern.

A straightforward relationship exists between the orientation tensor and the susceptibility tensor (see *Ježek and Hrouda, 2000*)

$$\mathbf{k} = K\mathbf{I} + \Delta\mathbf{E} \ , \tag{6}$$

where **k** is rock susceptibility tensor and **I** is identity matrix. For prolate spheroids, $K = K_2 = K_3$, $\Delta = K_1 - K$ ($K_1 \geq K_2 \geq K_3$ are grain principal susceptibilities) and **E** is orientation tensor of grain maximum susceptibility axes. For oblate spheroids, $K = K_1 = K_2$, $\Delta = K - K_3$ and **E** is orientation tensor of grain minimum susceptibility axes.

The representation of the mineral preferred orientation through the orientation tensor, which is the symmetric second rank tensor, may seem to be an oversimplified approach with respect to the possible complexities of the natural fabrics known from X-ray pole figure goniometry or electron backscatter diffraction. However, one should realize that the AMS measured in weak magnetic fields, in which the magnetization is directly proportional to the magnetizing field, is also represented by the symmetric second rank susceptibility tensor and cannot in principle provide us with the information of partial maxima or minima. From this point of view, the use of the orientation tensor is adequate for the sake of correlation of the mineral preferred orientation and the AMS.

3. GRAIN AMS OF MD AND SD PARTICLES

In MD ferromagnetic substances, the external magnetizing field is modified within each particle by the demagnetizing field and Eq. (1) can then be modified as follows

$$\boldsymbol{M} = \boldsymbol{\kappa}\boldsymbol{H}_{eff} = \boldsymbol{\kappa}\left(\boldsymbol{H} - \mathbf{N}\boldsymbol{M}\right) \ , \tag{7}$$

where $\boldsymbol{\kappa}$ is tensor of true or intrinsic susceptibility, $\boldsymbol{H}_{eff}$ is vector of the intensity of effective magnetizing field within particle, and **N** is tensor of demagnetizing factor solely depending on the particle shape (e.g., *Osborn, 1945*; *Stoner, 1945*; *Coe, 1966*; *Newell et al., 1993*). Then, the tensor of apparent susceptibility of the MD mineral of magnetite (titanomagnetite) type, which is magnetically isotropic in weak magnetic fields, is as follows (e.g., *Nagata, 1961*; *Uyeda et al., 1963*; *Stacey and Banerjee, 1974*; *Jelínek, 1993*)

$$\mathbf{K} = \kappa\left(\mathbf{I} + \kappa\mathbf{N}\right)^{-1} , \tag{8}$$

where κ is the isotropic intrinsic susceptibility and **I** is identity matrix.

Figure 1 shows the apparent vs. intrinsic susceptibility plot for spherical particle. For $\kappa < 0.1$ the apparent susceptibility virtually equals the intrinsic one. With increasing κ, the

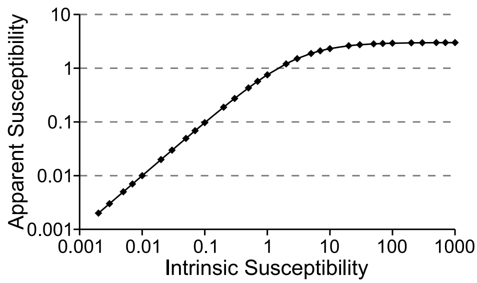

Fig. 1. Relationship between apparent and intrinsic susceptibilities for spherical particles.

apparent susceptibility increases more slowly, and at $\kappa > 100$, the apparent susceptibility no longer increases with increasing intrinsic susceptibility, infinitesimally approaching 3. Unfortunately, the intrinsic susceptibility of magnetite (titanomagnetite) is only poorly known, because it can be measured only by special permeameters avoiding self-demagnetizing effects (*Stacey and Banerjee, 1974, p. 71*), which are not frequent in rock magnetism laboratories. Nevertheless, the existing data indicates that it varies likely from 5 to 20 (*Parry, 1965*; *Stacey and Banerjee, 1974*; *Janák, 1977*; *Hartstra, 1982*; *Dunlop, 1984*; *Dunlop and Özdemir, 1997*).

The components of the grain tensor of the apparent susceptibility of magnetite (titanomagnetite) ellipsoidal particle in the coordinate system of particle axes ($a \geq b \geq c$) are

$$K_{11} = \frac{\kappa}{1+\kappa N_a}, \quad K_{22} = \frac{\kappa}{1+\kappa N_b}, \quad K_{33} = \frac{\kappa}{1+\kappa N_c}, \qquad (9)$$
$$K_{12} = K_{21} = K_{23} = K_{32} = K_{13} = K_{31} = 0 .$$

N_a, N_b and N_c are the demagnetizing factors along the respective grain axes. Figure 2 shows the relationship between the grain degree of AMS and grain aspect ratio for prolate spheroids as a function of intrinsic susceptibility. It is obvious that the degree of grain AMS increases both with grain aspect ratio and intrinsic susceptibility. From Eq. (9) it follows that the shape of the AMS ellipsoid is similar to that of the ellipsoidal grain, i.e. the maximum susceptibility is parallel to the maximum grain axis, the same relationship holding for the minimum axes.

Hargraves et al. (1991), *Stephenson (1994)*, *Grégoire et al. (1995, 1998)* and *Cañon-Tapia (1996, 2001)* have shown that the AMS of volcanic rocks can be carried not only by mutually non-interacting anisometric grains of ferromagnetic minerals, but also by clusters of interacting grains, which can be even spherical, and called this phenomenon as distribution anisotropy. They also stated that the degree of AMS of these clusters can be significantly higher than that of individual grains. In 1D and 2D clusters, the degree of AMS may reach $P \approx 2$ (*Stephenson, 1994*), while in 3D clusters it may reach $P \approx 4$ (*Cañon-Tapia, 1996*).

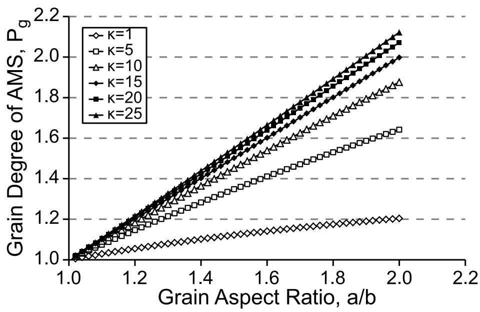

Fig. 2. Relationship between the grain degree of anisotropy of magnetic susceptibility and grain aspect ratio for prolate spheroids for varying intrinsic susceptibility values κ.

In SD magnetite (titanomagnetite) particles, the situation is quite different. If the particle is magnetized along its easy axis, no additional magnetization is induced, because the particle is already saturated along this direction; the susceptibility in that direction is effectively zero. If the particle is magnetized perpendicular to the easy axis (this direction is henceforth denoted by subscript $\perp$), the magnetization can slightly rotate toward the field in such a way that the component of magnetization in the hard direction is proportional to the internal field component in that orientation; the susceptibility is non-zero. The intrinsic susceptibility along this direction is (*Dunlop and Özdemir, 1997*)

$$\kappa_\perp = \frac{\mu_0 M_s^2}{2K_a} = \frac{M_s}{H_k} \ , \tag{10}$$

where μ_0 is permeability of free space, M_s is saturation magnetization, K_a is anisotropy constant and $H_k = 2K_a / \mu_0 M_s$ is microscopic coercivity related to macroscopic coercivity (H_c) as $H_k = 2.09 H_c$ (*Worm, 1998*; *Worm and Jackson, 1999*). The apparent susceptibility then is (*Hartstra, 1982*)

$$K_\perp = \frac{\kappa_\perp}{1 + \kappa_\perp N_b} \ . \tag{11}$$

The components of the grain tensor of the apparent susceptibility of magnetite (titanomagnetite) prolate spheroidal SD particle in the coordinate system of particle axes ($a \geq b \geq c$) are

$$K_{11} = 0 \,, \quad K_{22} = K_\perp \,, \quad K_{33} = K_\perp \,, \quad K_{12} = K_{21} = K_{23} = K_{32} = K_{13} = K_{31} = 0 \,. \tag{12}$$

In oblate particles, in which the spontaneous magnetization freely rotates in the plane perpendicular to the particle axis (see *Dunlop and Özdemir, 1997*), the same components are

$$K_{11} = 0 \,, \quad K_{22} = 0, \quad K_{33} = K_\perp \,, \quad K_{12} = K_{21} = K_{23} = K_{32} = K_{13} = K_{31} = 0 \,. \tag{13}$$

4. MODELS OF MAGNETIC FABRICS OF ENSEMBLES OF PARTICLES

Our investigation will be made using a very simple model considering an ensemble of magnetite/titanomagnetite grains (or their clusters) disseminated in the matrix of zero susceptibility. The grains have more or less the same shape, but show continuous distribution in size ranging from very small (SD) to slightly bigger (MD). Hence, the magnetic particles create one population from the mechanical point of view, but two sub-populations from the magnetic point of view. It is assumed that the preferred orientation of the grain axes originated during one process (for instance during lava flow), thus being represented by the same orientation tensor (and its I and T_e parameters) in MD and SD particles. There is no reason for the particles to change either their orientation or grain shape on the threshold of the existence of SD states.

The model rock susceptibility tensor in external coordinate system is

$$\mathbf{k} = p\sum\left(\mathbf{R}' \cdot \mathbf{K} \cdot \mathbf{R}\right) , \tag{14}$$

where p is percentage of magnetic mineral in rock, **K** is grain/cluster susceptibility tensor in the particle coordinate system and **R** is orientation matrix specifying grain/cluster orientation in the external coordinate system and consisting of direction cosines of grain axes and **R′** matrix is the transpose of the matrix **R.**

In MD particles, one can calculate the grain apparent susceptibility tensor from intrinsic susceptibility and demagnetizing factor (shape of the grain) using Eq. (9). Figure 3, which was constructed considering the magnetite intrinsic susceptibility of $\kappa = 20$, shows the variation of the degree AMS of the model according to I parameter for several values of the grain aspect ratio (a/b). It is obvious that the model degree of AMS increases with increasing grain aspect ratio and with increasing intensity of the orientation of particle axes. The maximum susceptibility direction is parallel to that of maximum concentration of particle axes.

In clusters of MD particles, one can calculate the cluster AMS using the equations by *Stephenson (1994)* or *Cañon-Tapia (1996)* who also present corresponding graphs.

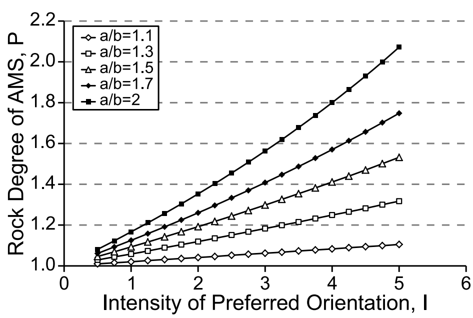

Fig. 3. Model of the variation of the degree of anisotropy of magnetic susceptibility of the ensemble of magnetite multi-domain particles (prolate spheroids) with the I parameter for several values of the grain aspect ratio (a/b).

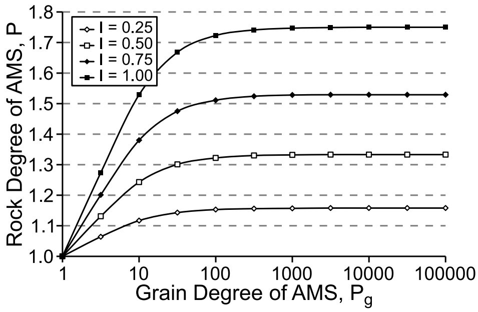

Fig. 4. Model relationship between the rock degree of anisotropy of magnetic susceptibility and grain degree of anisotropy of magnetic susceptibility for varying intensity of the preferred orientation, *I*, of the axes of prolate spheroids of equal size.

However, as the cluster AMS corresponds to the AMS of strongly elongated grains, it is from the purely formal point of view in the frame of our modelling sufficient, to work with the grain AMS, only (i.e., to consider clusters as elongated grains). Even though it is not possible to explicitly present it in terms of P_g parameter, the grain degree of AMS of SD particles is no doubt extremely large (see Eqs (12) and (13)). *Hrouda (1980)* showed that the degree of AMS of the rock whose AMS is carried by very strongly anisotropic grains ($P_g > 100$) is solely controlled by the preferred orientation of the grains (for illustration see Fig. 4). We can use this property in modelling the AMS of an ensemble of SD particles.

In SD particles, one can calculate the grain apparent susceptibility tensor from Eqs (10)–(13). Figure 5, which was constructed considering $M_s = 480$ kA/m and $K_a = 2.5 \times 10^4$ J m^3 for magnetite (*Dearing et al., 1996*; *Dunlop and Özdemir, 1997*), shows the variation of the degree AMS of the model containing the SD particles according to *I* parameter. Even though the curves were calculated for various grain aspect ratios and therefore also for various N_b in Eq. (11), only one curve is presented in Fig. 5, because the

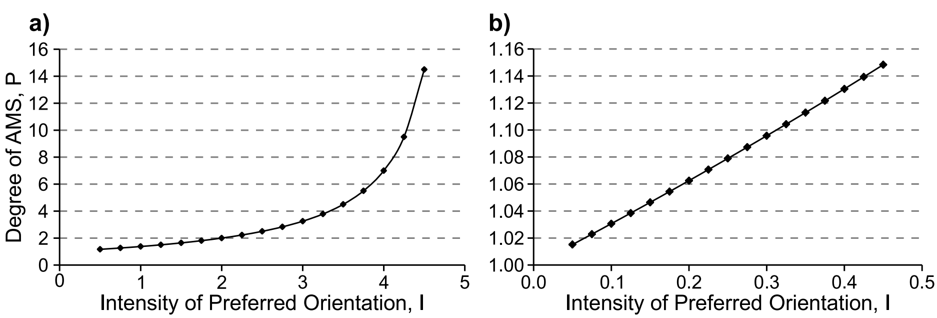

Fig. 5. Model of the variation of the degree of anisotropy of magnetic susceptibility of the ensemble of uniaxial single-domain magnetite particles with **a)** *I* parameter ranging widely (from 0.5 to 4.5), and **b)** an order-of magnitude less (from 0.05 to 0.45).

differences between individual curves were so small that they could not be illustrated graphically. It is obvious that the model degree of AMS increases with increasing intensity of the orientation of particle axes. The maximum susceptibility is then parallel to the maximum concentration of the shortest particle axes and the minimum susceptibility is parallel to the maximum concentration of the longest axes (*Stephenson et al., 1986*). If the *I* parameter range is used similarly to that used in MD particles, the rock degree of AMS is mostly unrealistically high (Fig. 5a). To obtain realistic values, one has to consider values of the *I* parameter that are orders of magnitude lower (Fig. 5b).

Using the same conceptual framework as that by *Henry (1983)*, *Henry and Daly (1983)*, *Cañon-Tapia (2001)* and *Ferré (2002)*, and realizing that each susceptibility tensor can be resolved into the mean susceptibility and the normed susceptibility tensor, the susceptibility tensor of the model consisting of both MD and SD particles, whose axes have the same orientations, can be written

$$\mathbf{k} = c_{MD}\,{}^{MD}K_m\,{}^{MD}\mathbf{k}_n + c_{SD}\,{}^{SD}K_m\,{}^{SD}\mathbf{k}_n \;, \tag{15}$$

where ${}^{MD}\mathbf{k}_n$ and ${}^{SD}\mathbf{k}_n$ are normed suscetibility tensors of MD and SD fractions, respectively, ${}^{MD}K_m$ and ${}^{SD}K_m$ are mean susceptibilities of MD and SD fractions, respectively, and c_{MD} and c_{SD} are percentages of MD and SD particles, respectively. It is worth to note that the mean susceptibilities of the MD and SD particles differ. Figure 6a shows the variation of the degree AMS of the model according to c_{SD} parameter ($c_{MD} = 1 - c_{SD}$) for constant M_s (480 kA/m) and several values of the *I* parameter and grain aspect ratio. It is obvious that the degree of AMS of the model initially decreases with increasing SD particle content and the maximum susceptibility direction is parallel to that of maximum concentration of particle axes (normal magnetic fabric). After reaching the lowest value, the degree of AMS of the model increases again and it is the minimum susceptibility direction that is parallel to that of maximum concentration of particle axes (inverse magnetic fabric). Figure 6b shows the same variation for constant $I = 1$ and $a/b = 2$ and variable *Ms* (ranging from 100 kA/m through 200–400 kA/m to 500 kA/m). The variations are very similar to those of Fig. 6a.

In the models presented in Fig. 6a,b, all the MD and SD particles are equal (MD grains have the same intrinsic susceptibility, SD the same saturation magnetization, and both SD and MD have the same aspect ratio and the same orientation tensor). This simplification enables us to evaluate the bulk susceptibility using the relation between susceptibility and orientation tensor, Eq. (6). To suppress a suspicion that the model is oversimplified, we present in Fig. 6c a more complex example. We model a multiparticle system composed from a large number of similar but unequal prolate MD and SD particles (together 2000 particles) that from an initial random orientation were reoriented by plane strain ($I = 1$). Final orientation of the particles is shown in the lower area projection (SD particles marked by dots, MD by circles; elongation axis of plane strain is parallel to the *x*-axis). Aspect ratios of both SD and MD were randomly generated from the normal distribution $N\left(2, 0.3^2\right)$, effectively ranging from 1.4 to 2.6. Similarly, intrinsic susceptibilities of MD particles were randomly chosen between 10 and 30, and SD saturation magnetization was between 150 and 350 kA/m. As the particles are unequal, the previous approach based on the orientation tensor cannot be used. Individual particles rotate differently (according to their aspect ratio) and the bulk susceptibility must be computed by summing up all rotated individual (magnetically unequal) particles. Software by *Ježek and Hrouda (2002)* was adapted to do the task and the bulk susceptibility was repeatedly evaluated for variable percentage of SD particles. The resulting curve of the parameter *P* shown in Fig. 6c is very similar to the previous ones (Fig. 6b). Small squares on the curve indicate concentrations for which the first eigenvector of bulk susceptibility is computed and plotted in the stereogram. For low concentrations of SD the first eigenvector is parallel to plane strain main axis and switches into a perpendicular direction when SD concentration becomes higher. Additional modelling showed that the character of the *P* curve does not change if SD particles have different distribution of aspect ratios than MD (for example, SD are less prolate). This is valid also if we allow the MD and SD subfabrics to have differently oriented maxima. For a difference $\sim 20^{o}$, the transition from MD to SD dominated fabric (from normal to inverse fabric) is still well visible on the *P* curve, although the minimum is not so well pronounced.

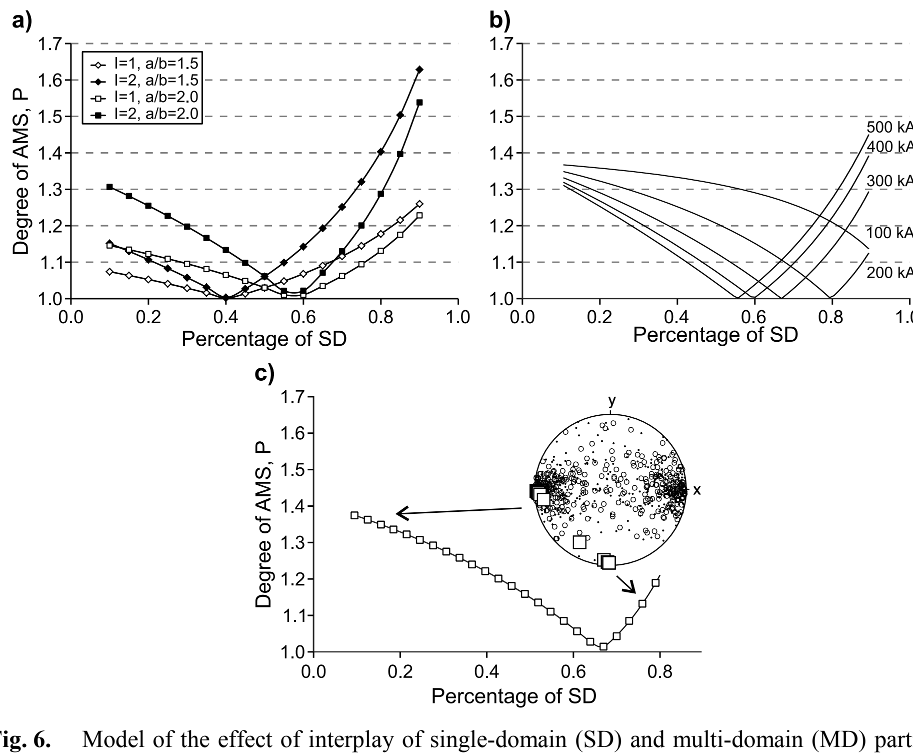

Fig. 6. Model of the effect of interplay of single-domain (SD) and multi-domain (MD) particles on the resultant degree of anisotropy of magnetic susceptibility for **a)** constant saturation magnetization M_S (480 kA/m) and variable intensity of the preferred orientation (I) and the grain aspect ratio (a/b), **b)** constant $I = 1$ and $a/b = 2$ and variable M_S, and **c)** for random distribution of parameters (see text for explanation).

In addition to plane strain, we also considered predominating flattening or constriction. Even though there are differences in detail, the general trends are similar regardless of the deformation considered.

5. IMPLICATIONS OF THE MODEL FOR ASSESSING THE EFFECT OF SD PARTICLES

At present, there is no universal tool in the low-field AMS how to assess the effect of SD particles on the whole rock AMS quantitatively. Only partial solutions exist. If the rock investigated shows the inverse fabric, one can measure the AMS and AMR or the AMS and HFA. If the AMS fabric and AMR (HFA) fabric are antiparallel, i.e. K_3 in AMS is parallel to K_1 in AMR (HFA) and K_1 in AMS is parallel to K_3 in AMR (HFA), the inverse magnetic fabric is likely due to the prevailing effect of the SD particles in the rock. If the fabrics are parallel, i.e. K_3 in AMS is parallel to K_3 in AMR (HFA) and K_1 in AMS is parallel to K_1 in AMR (HFA), the inverse fabric is likely due to geological reasons. Examples of the use of these techniques are presented in *Chadima et al. (2005)* and *Almqvist et al. (2012)*.

Another partial solution based on the results of the above modelling is as follows. If the rock AMS is carried by a mineral that shows measurable variation of its susceptibility with magnetizing field (for example, titanomagnetite), one can investigate also the field variation of the AMS and determine the AMS of the MD fraction (see *Hrouda, 2009*). After comparing it with the whole rock AMS, one can assess the effect of SD fraction on the whole rock AMS. Two small groups of specimens of volcanic and dyke rocks can illustrate this technique. The first group consists of two specimens of basalts from Hawaii, provided by Dr. Carsten Vahle, and of two specimens of ignimbrites from the Western Carpathians, provided by Dr. Emö Márton. The dominating susceptibility carrier is titanomagnetite in all of them. The AMS of these specimens was measured in variable low-fields and the AMS of the MD titanomagnetite fraction was then calculated using the method by *Hrouda (2009)*. This was possible, because all the specimens show conspicuous linear dependence between susceptibility and magnetizing field in the field interval 50–400 A/m (Fig. 7a). In basalt specimens (SR 720 and SR 719), the degree of AMS of the whole rock is relatively similar to the degree of AMS of the MD fraction (Fig. 7b). It is likely that the whole rock AMS is dominantly carried by the MD fraction and the effect of the SD fraction is small. On the other hand, in ignimbrite specimens (BO 4459 and BO 4460), the whole rock degree of AMS is very low, much lower than the degree of AMS of the MD fraction (Fig. 7b). According to the personal information by Dr. E. Márton, the ignimbrite contains large amount of SD particles in its ferromagnetic fraction revealed by the investigation of hysteresis properties. As the AMS of the SD fraction shows the inverse orientation with respect to the AMS of MD ferromagnetic fraction (*Stephenson et al. 1986*; *Ferré 2002*), this may explain relatively high degree of AMS of the MD ferromagnetic fraction and very low degree of AMS of the whole rock.

The second group consists of 14 specimens of volcanic and dyke rocks (camptonite, bostonite, trachybasalt) from several localities of the České Středohoří Mountains, which were provided by Dr. Martin Chadima. In this group, one can find specimens in which the degree of AMS of the whole rock and of the MD ferromagnetic fraction are similar

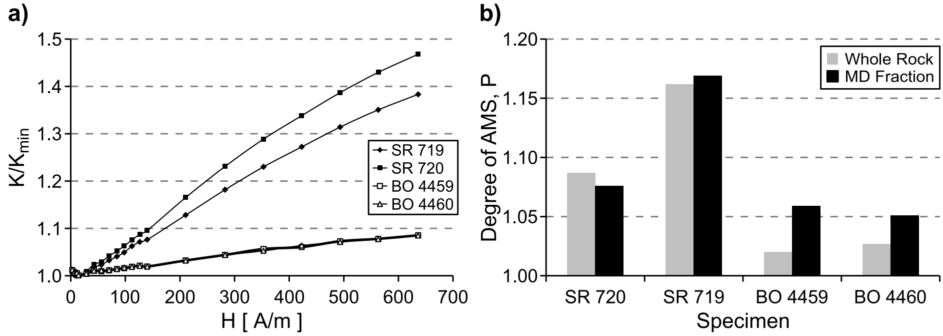

Fig. 7. **a)** Field variation of normalized susceptibility (K/K_{min}) and **b)** column diagram of the degree of anisotropy of magnetic susceptibility (*P*) of the whole rock and of the multi-domain ferromagnetic fraction for basalt and ignimbrite.

(specimens CS 18/10/2, CS 27/02/2, see Fig. 8a) and the effect of the SD fraction is small; the AMS and AMR fabrics in localities CS 18 and CS 27 are very well coaxial (Fig. 8b,c). On the other hand, there are specimens in which the degree of AMS of the MD ferromagnetic fraction is much higher than that of the whole rock (specimens CS 32/24/2, CS 33/02/1, CS 39/14/01, CS 44/01/1). In these specimens, the effect of the SD fraction on the whole rock AMS is strong, diminishing it. In locality CS 32, the AMS fabric is inverse with respect to the AMR fabric (Fig. 8d), in localities CS 33 and CS 39, $^{\mathrm{AMS}}k_3$ and $^{\mathrm{AMR}}k_3$ are parallel, while $^{\mathrm{AMS}}k_1$ and $^{\mathrm{AMR}}k_1$ are perpendicular (Fig. 8e). One may in this way assess the effect of the SD particles on the whole rock AMS.

6. DISCUSSION

Our modelling shows that the degree of AMS of ensemble of preferably oriented SD particles is much higher than that of ensemble of MD particles possessing the same particle shapes and the same intensity of preferred orientation. This might imply existence of prevailing inverse magnetic fabrics provided that the rocks contain MD and SD particles in comparable amounts. However, the reality is very different, the occurrence of inverse magnetic fabrics due to SD particles is in the most rocks rather exception than a rule. In fact, the inverse magnetic fabrics due to SD particles were identified only in some volcanic rocks, whose magnetic particles may partially be really small obeying the condition for existence of SD particles (e.g., *Stephenson et al., 1997*; *Worm and Jackson, 1999*; *Chadima et al., 2009*). *Cañon-Tapia and Mendoza-Borunda (2014)* even deny the existence of the inverse fabric due to SD particles at all and present a number of arguments for that. On the other hand, there are AMS fabrics evidently inverse to the AMR fabrics (e.g., *Chadima et al., 2009*) as well as the low-field AMS fabrics inverse to the HFA fabrics (*Almqvist et al., 2012*), which is in contradiction to the *Cañon-Tapia and Mendoza-Borunda (2014)* view. Considering all these facts we can conclude that the amounts of SD particles are in general very low.

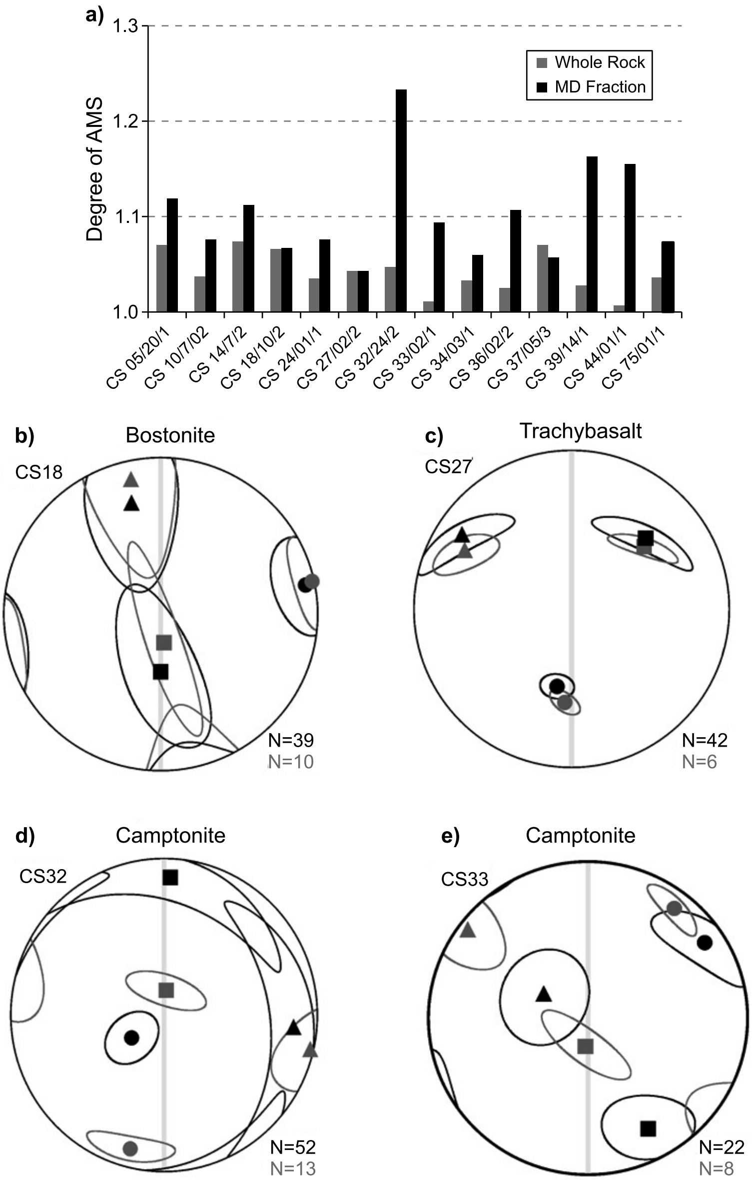

Fig. 8. **a)** Column diagram of the whole rock degree of anisotropy of magnetic susceptibility (AMS) and multi-domain (MD) ferromagnetic fraction degree of AMS for volcanic and dyke rocks, and **b)–e)** principal directions of locality mean tensors with respective confidence areas for the same rocks. The figures b)–e) are equal-area plots on lower hemisphere and were adapted from *Chadima et al. (2009)*. In b)–e): ■ – maximum direction, ▲ – intermediate direction, ● – minimum direction; black symbols represent anisotropy of magnetic susceptibility, grey symbols represent anisotropy of magnetic remanence.

The degree of AMS of volcanic rocks is generally low (for summary see *Hrouda, 1982*; *Tarling and Hrouda, 1993*; *Cañon-Tapia, 2004, 2011*), being lower in low viscosity lavas than in high viscosity ones (*Hrouda et al., 2005*). The low degree of AMS in volcanic rocks is commonly explained by assuming the flowing lava being relatively ineffective in orientating magnetic particles (for review see *Tarling and Hrouda, 1993*; *Cañon-Tapia, 2004*). In addition, *Hrouda et al. (1994)* found out in their modelling studies that if the lava flow resembles simple shear movement in terms of strain, the intensity of the preferred orientation of particles may exhibit oscillatory motions with increasing strain and the degree of AMS behaves in the same way. Our modelling adds the third possible cause of the low degree of AMS, i.e. the simultaneous effect of MD and SD particles. This is well illustrated by Fig. 6 showing that the effect may in some cases give rise to really low degree of AMS. As lavas can in general cool relatively rapidly, at least a part of ferromagnetic minerals can be very small (SD) resulting in non-negligible effect of these particles.

The investigation of the field variation of the AMS in the fields of the Rayleigh law range provides us with the field-independent and field-dependent AMS components (*Hrouda, 2009*). While the former component can be controlled by various factors, the latter component is solely the MD phenomenon. By comparing the field-dependent AMS component to the whole-rock AMS, the fabric of SD particles can be roughly assessed. Using the MFK1-FA Kappabridge or the KLY5-A Kappabridge equipped with the 3D rotator, the measurement of the field variation can be automated (*Studýnka et al., 2014*), thus enabling large collections of specimens to be easily measured.

7. CONCLUSIONS

Using simple mathematical models, the role of single-domain (SD) magnetic particles was investigated in creation of inverse magnetic fabrics. The modelling has brought the following conclusions:

1. The anisotropy of magnetic susceptibility (AMS) of multi-domain (MD) titanomagnetite fraction is controlled by the grain shape and intrinsic susceptibility and the intensity of the preferred orientation of the grains. On the other hand, the AMS of SD fraction is controlled by the intrinsic susceptibility in the direction perpendicular to the easy axis and by the intensity of the preferred orientation of the particles.
2. The degree of AMS of ensemble of preferably oriented SD particles is much higher than that of the ensemble of MD particles showing the same preferred orientation. This would imply existence of frequent inverse magnetic fabrics. However, the occurrence of inverse magnetic fabrics due to SD particles is rather exception than a rule. Consequently, the amounts of SD particles must be in general low.
3. The presence of SD particles in the amount insufficient for creation of an inverse magnetic fabric may nevertheless diminish the whole rock AMS. It can be one of the reasons for relatively low AMS in volcanic rocks whose magnetic particles may be really small obeying the condition for existence of SD particles.
4. The role of SD particles in controlling the whole rock AMS can be assessed through investigation of both AMS and anisotropy of magnetic remanence (AMR),

through investigation of field-dependent AMS, or through investigation of high-field (torque) magnetic anisotropy (HFA).

Acknowledgements: Drs. Emö Márton, Carsten Vahle, and Martin Chadima are thanked for providing us with specimens of ignimbrite, basalt, and volcanic and dyke rocks, respectively. The research was supported financially by the Czech Science Foundation (15-18154S).

References

Almqvist B.S.G., Bosshard S.A., Hirt A.M., Mattsson H.B. and Hetenyi G., 2012. Internal flow structures in columnar joited basalt from Hreppholar, Iceland: II. Magnetic anisotropy and rock magnetic properties. *Bull. Volcanol.*, **74**, 1667–1681, DOI: 10.1007/s00445-012-0622-0.

Borradaile G.J. and Gauthier D., 2001. AMS-detection of inverse fabrics without AARM, in ophiolite dikes. *Geophys. Res. Lett.*, **28**, 3517–3520.

Cañon-Tapia E., 1996. Single-grain versus distribution anisotropy: a simple three-dimensional model. *Phys. Earth Planet. Inter*., **94**, 149–158.

Cañon-Tapia E., 2001. Factors affecting the relative importance of shape and distribution anisotropy in rocks: theory and experiments. *Tectonophysics*, **340**, 117–131.

Cañon-Tapia E., 2004. Anisotropy of magnetic susceptibility of lava flows and dykes: A historical account. In: Martin-Hernandez F., Luneburg C.M., Aubourg C. and Jackson M. (Eds), *Magnetic Fabric: Methods and Applications*. Geological Society, London, Special Publications, **238**, 205–225.

Cañon-Tapia E., 2011. AMS in granites and lava flows: Two end members of a continuum? In: Petrovský E., Herrero-Bervera E., Harinarayana T. and Ivers D. (Eds), *The Earth's Magnetic Interior*. IAGA Special Sopron Book Series I. Springer-Verlag, Heidelberg, Germany, 263–280.

Cañon-Tapia E. and Mendoza-Borunda R., 2014. Magnetic petrofabric of igneous rocks: Lessons from pyroclastic density current deposits and obsidians. *J. Volcanol. Geotherm. Res.*, **289**, 151–169.

Cañon-Tapia E., Walker G.P.L. and Herrero-Bervera E., 1994. Magnetic fabric and flow direction in basaltic Pahoehoe lava of Xitle Volcano, Mexico. *J. Volcanol. Geotherm. Res.*, **65**, 249–263.

Chadima M., Cajz V. and Týcová P., 2009. On the interpretation of normal and inverse magnetic fabric in dikes: examples from the Eger Graben, NW Bohemian Massif. *Tectonophysics*, **466**, 47–63.

Coe R.S., 1966. Analysis of magnetic shape anisotropy using second-rank tensors. *J. Geophys. Res.*, **71**, 2637–2644.

Dragoni M., Lanza R. and Tallarico A., 1997. Magnetic anisotropy produced by magma flow: theoretical model and experimental data from Ferrar dolerite sills (Antarctica). *Geophys. J. Int.*, **128**, 230–240.

Dunlop D.J., 1984. A method of determining demagnetizing factor from multidomain hysteresis. *J. Geophys. Res.*, **89**, 553–558.

Dunlop D.J. and Özdemir Ö., 1997. *Rock Magnetism. Fundamentals and Frontiers*. Cambridge University Press, Cambridge, U.K., 573 pp.

Ernst R.E. and Baragar W.R.A., 1992. Evidence from magnetic fabric for the flow pattern of magma in the Mackenzie giant radiating dyke swarm. *Nature*, **356**, 511–513.

Ferré E.C., 2002. Theoretical models of intermediate and inverse AMS fabrics. *Geophys. Res. Lett.*, **29**, 1127, DOI: 10.1029/2001GL01436.

Graham J.W., 1966. Significance of magnetic anisotropy in Appalachian sedimentary rocks. In: Steinhart J.S. and Smith T.J. (Eds), *The Earth beneath the Continents*. Geophysical Monograph Series, **10**, American geophysical Union, Washington, D.C., 627–648.

Grégoire V., de Saint Blanquat M., Nedelec A. and Bouchez J.-L., 1996. Shape anisotropy versus magnetic interactions of magnetic grains: experiments and application to AMS in granitic rocks. *Geophys. Res. Lett*., **18**, 2193–2196.

Grégoire V., Darrozes J., Gaillot P., Nedelec A. and Launeau P., 1998. Magnetite grain fabric and distribution anisotropy vs. rock magnetic fabric: a three-dimensional case study. *J. Struct. Geol.*, **20**, 937–944.

Hartstra R.L., 1982. Grain-size dependence of initial susceptibility and saturation magnetization-related parameters of four natural magnetites in the PSD-MD range. *Geophys. J. R. Astr. Soc*., **761**, 447–495.

Henry B., 1983. Interpretation quantitative de l'anisotropie de susceptibilité magnétique. *Tectonophysics*, **91**, 165–177 (in French).

Henry B. and Daly L., 1983. From qualitative to quantitative magnetic anisotropy analysis: the prospect of finite strain calibration. *Tectonophysics*, **98**, 327–336.

Hrouda F., 1980. Magnetocrystalline anisotropy of rocks and massive ores: a mathematical model study and its fabric implications. *J. Struct. Geol.*, **2**, 459–462.

Hrouda F., 1982. Magnetic anisotropy of rocks and its application in geology and geophysics. *Geophys. Surv.*, **5**, 37–82.

Hrouda F., 2009. Determination of field-independent and field-dependent components of anisotropy of susceptibility through standard AMS measurements in variable low fields I: Theory. *Tectonophysics*, **466**, 114–122.

Hrouda F., Melka R. and Schulmann K., 1994. Periodical changes in fabric intensity during simple shear deformation and its implications for magnetic susceptibility anisotropy of sedimentary and volcanic rocks. *Acta Univ. Carol. Geol.*, **38**, 37–56.

Hrouda F., Chlupáčová M. and Novák J.K., 2002. Variations in magnetic anisotropy and opaque mineralogy along a kilometer deep profile within a vertical dyke of the syenogranite porphyry at Cínovec (Czech Republic). *J. Volcanol. Geotherm. Res.*, **113**, 37–47.

Hrouda F., Chlupáčová M., Schulmann K., Šmíd J. and Závada P., 2005. On the effect of lava viscosity on the magnetic fabric intensity in alkaline volcanic rocks. *Stud. Geophys. Geod.*, **49**, 191–212.

Ihmlé P.F., Hirt A., Lowrie W. and Dietrich D., 1989. Inverse magnetic fabric in deformed limestones of the Morcles nappe, Switzerland. *Geophys. Res. Lett*., **16**, 1383–1386.

Janák F., 1977. The determination of the content of ferromagnetic minerals in rock sample. *Sborník geologických věd (J. Geol. Sci.)*, **14**, 153–164.

Jelínek V., 1981. Characterization of magnetic fabric of rocks. *Tectonophysics*, **79**, T63–T67.

Ježek J. and Hrouda F., 2000. The relationship between the Lisle orientation tensor and the susceptibility tensor. *Phys. Chem. Earth A*, **25**, 469–474.

Lisle R.J., 1985. The use of the orientation tensor for the description and statistical testing of fabrics. *J. Struct. Geol.*, **7**, 115−117.

Nagata T., 1961. *Rock Magnetism*. Maruzen, Tokyo, Japan.

Newell A.J., Williams W. and Dunlop D.J., 1993. A generalization of the demagnetizing tensor for nonuniform magnetization. *J. Geophys. Res.*, **98**, 9551−9555.

Osborn J.A., 1945. Demagnetizing factors of the general ellipsoid. *Phys. Rev.*, **67**, 351−357.

Owens W.H., 1974. Mathematical model studies on factors affecting the magnetic anisotropy of deformed rocks. *Tectonophysics*, **24**, 115−131.

Parry L.G., 1965. Magnetic properties of dispersed magnetic powders. *Phil. Mag.*, **11**, 303−312.

Raposo M.I.B. and Ernesto M., 1995. Anisotropy of magnetic susceptibility in the Ponta Grossa dyke swarm (Brazil) and its relationship with magma flow direction. *Phys. Earth Planet. Inter.*, **87**, 183−196.

Rochette P., 1988. Inverse magnetic fabric in carbonate-bearing rocks. *Earth Planet. Sci. Lett.*, **90**, 229−237.

Rochette P., Aubourg C. and Perrin M., 1999. Is this magnetic fabric normal? A review and case studies in volcanic formations. *Tectonophysics*, **307**, 219−234.

Rochette P., Jackson M. and Aubourg C., 1992. Rock magnetism and the interpretation of anisotropy of magnetic susceptibility. *Rev. Geophys*., **30**, 209−226.

Scheidegger A.E., 1965. On the statistics of the orientation of bedding planes, grain axes, and similar sedimentological data. *U.S. Geol. Surv. Prof. Pap.*, 525-C, 164−167.

Stacey F.D. and Benerjee S.K., 1974. *The Physical Principles of Rock Magnetism*. Elsevier, Amsterdam, The Netherlands, 195 pp.

Stephenson A., 1994. Distribution anisotropy: two simple models for magnetic lineation and foliation. *Phys. Earth Planet. Inter.*, **82**, 49-53.

Stephenson A., Sadikun S. and Potter D.K., 1986. A theoretical and experimental comparison of the anisotropies of magnetic susceptibility and remanence in rocks and minerals. *Geophys. J. R. Astr. Soc*., **84**, 185−200.

Stoner E.C., 1945. The demagnetizing factors for ellipsoid. *Phil. Mag*., **36**, 803−820.

Studýnka J., Chadima M. and Suza P., 2014. Fully automated measurement of anisotropy of magnetic susceptibility using 3D rotator. *Tectonophysics*, **629**, 6−13.

Tarling D.H. and Hrouda F. 1993. *The Magnetic Anisotropy of Rocks*. Chapman & Hall, London, U.K., 217 pp.

Uyeda S., Fuller M.D., Belshé J.C. and Girdler R.W., 1963. Anisotropy of magnetic susceptibility of rocks and minerals. *J. Geophys. Res.*, **68**, 279−292.

Worm H.-U., 1998. On the superparamagnetic - stable single domain transition for magnetite, and frequency dependence of susceptibility. *Geophys. J. Int*., **133**, 201−206.

Worm H.-U. and Jackson M., 1999. The superparamagnetism of Yucca Mountain Tuff. *J. Geophys. Res.*, **104**, 25415−25425.

Winkler A., Florindo F. and Sagnotti L., 1996. Inverse to normal magnetic fabric transition in an upper Miocene marly sequence from Tuscany, Italy. *Geophys. Res. Lett.*, **23**, 909−912.